Structural diversity of frameshifting signals : reprogramming the programmed

Yu, C.H.

Chapter Ⅱ

Structural diversity of RNA structures involved in programmed ribosomal frameshifting: a literature review

Introduction

Messenger ribonucleic acid or mRNA is defined as the medium of information flow from deoxyribonucleic acid (DNA) into proteins and needs to be decoded in a string of non-overlapping codons into amino acids by ribosomes. During this process, called translation, the reading frame of codon triplets is strictly maintained to ensure synthesis of the correct protein. However, in addition to the standard rule of decoding, several alternative ways to decipher genetic information, namely recoding (1, 2), have been documented in all kingdoms of life.

Recoding, including translational bypassing, stop codon readthrough and stop codon redefinition, and programmed ribosomal frameshifting (PRF), is used by many organisms to regulate gene expression and/or to expand their gene expression repertoire. To compete with standard decoding, specific signals, sometimes in conjunction with *trans*-acting factors, should be embedded in the mRNA to promote recoding. The recoding signals in mRNA consist of two main elements: one is the sequence where the actual recoding takes place and the other is a stimulator. The stimulator affects directly or indirectly via RNA binding proteins translating ribosomes to alter their normal decoding behavior. Examples of such sequences are the pentanucleotide motif downstream of a stop codon which enhances near-cognate transfer RNA (tRNA) to compete with release factors from yeast to mammals (3–5) or the selenocysteine insertion element (SECIS), an elaborate RNA structure that is bound by specific protein co-factors, which is required for incorporation of the 21st amino acid, selenocysteine, at designated UAG stop codons (6–8).

1. Programmed ribosomal frameshifting

Programmed ribosomal frameshifting (PRF) is one of the most studied topics of recoding. During PRF ribosomes are "programmed" to switch the original reading frame at a so-called slip site by one nucleotide into the 3'-direction, named +1 PRF, or by one or two nucleotides into the 5'-direction, named -1 or -2 PRF, respectively, at a defined ratio. The different types of PRF require distinct recoding elements.

In the case of -2 PRF, which is rarely documented, bacteria phage Mu utilizes -2 PRF at C.GG_G.GG_C.GA_ (the underscores indicate the original reading frame while the dots denotes the frame after the shift) without identified stimulatory element to synthesize proteins involved in tail assembly (9).

+1 PRF has been found in both prokaryotes and eukaryotes and is responsible for the expression of certain important physiological genes. Most cases of +1 PRF found to date rely on RNA motifs to stall ribosomes on a slippery sequence (hungry codon) and/or generate tension on mRNA [Shine-Dalgarno (SD)-like sequences] to promote frameshifting towards the 3'-end (10). The paradigm of +1 PRF in prokaryotes is the

expression of *prfB* gene, encoding release factor 2 (RF2), in *Escherichia coli* (*E. coli*). Combination of three mRNA elements is important for *prfB* frameshifting. First, the in-frame UGA stop codon of the CUU_ U.GA_C. frameshift site is in a weak context to promote translation termination. Second, a SD-like sequence in optimal spacing upstream of the slip site (11, 12) interacts with 16S ribosomal RNA (rRNA) to build up tension on the mRNA. Finally, the identity of peptidyl-tRNA is critical, which means the peptidyl-tRNA has to re-pair to the codon after the +1 shift (13). In this case the 5'-GAG-3' anticodon of the tRNA-Leu retains base pairing with the UUU codon in the +1 frame. The synthesis of RF2 demonstrates an elegant autoregulatory mechanism (14) and the relative cellular abundance of RF2 may also correlate with UGA (re)definition (15).

Two retrotransposons, Ty1 and Ty3, of yeast *Saccharomyces cerevisiae* (*S. cerevisiae*) utilize +1 PRF to express essential genes but by different mechanisms. In Ty1, a low-abundance tRNA-Arg, which is encoded by a single-copy gene and decodes the rare ("hungry") AGG codon, plays a major role in inducing +1 PRF on a CUU_A.GG_C slippery sequence (16). This mechanism strongly resembles the case of *prfB* of *E. coli* as mentioned above. Ty3 uses a different way to achieve +1 PRF. A mechanism of out-of-frame binding of aminoacyl-tRNA was proposed. The frameshifting-inducing peptidyl-tRNA and a 14 nts stimulatory sequence immediately distal to the slippery sequence are suggested to be required for efficient +1 PRF (17), although the mechanism is still controversial (18).

The intracellular polyamine negative regulator, antizyme, is synthesized through +1 PRF by P-site tRNA slippage and this kind of regulation is conserved from yeast to mammals (19). The feedback regulation of polyamine levels by antizymes through +1 PRF is reminiscent of RF2 synthesis in *E.coli*, but the underlying mechanisms are somewhat different. An UGA stop codon in the A-site of UCC_U.GA_U. slippery sequence is responsible to stall ribosomes, as well as an upstream polyamine sensing element (20) and a downstream pseudoknot structure (in mammalian antizyme 1) (21). These elements synergistically promote P-site tRNA with anticodon 5'-GGA-3' to re-pair with the near-cognate CCU codon in the +1 reading frame. Although the role of the downstream pseudoknot is considered to stall ribosomes and proved to be insensitive to polyamine levels, a –1 PRF inducing pseudoknot from *Infectious bronchitis virus* (IBV) cannot replace it (22). Since a detailed analysis of the antizyme pseudoknot structure is still lacking, the specific differences between the two types of frameshifting pseudoknots still need to be determined. Recently, expression of antizyme in *S. cerevisiae* has been found to be regulated by prion [PSI^+], the aggregated (amyloid) form of release factor 3 (eRF3) (23). This and a related study (24) open a new vision of epigenetic control of such delicate gene regulation.

–1 PRF was demonstrated for the first time over 25 years ago to explain the expression of the overlapping *gag-pol* genes of *Rous sarcoma virus* (RSV) (25). Since then, numerous examples of -1 PRF in overlapping open reading frames (ORF) of eukaryotic RNA viruses, DNA and RNA bacteriophages, and bacterial insertion sequences and transposons have been found (26, 27). Although most of these cases are found in viruses or virus-like elements, one endogenous bacterial gene, *dnaX* (28), and three mammalian genes (29–31) so far have been shown to be expressed through -1 PRF, implying that -1 PRF may be involved in regulation of uncovered cellular genes in humans. Through sequence comparison and genetic analysis, a canonical -1 PRF regulating motif which contains two RNA elements has been identified: a heptameric slippery sequence where frameshifting occurs with the formulation of X_XX.Y_YY.Z (32) [for example, U_UU.U_UU.A in *gag-pol* junction of *Human immunodeficiency virus type-I* (HIV-1) (33)]; and an RNA structure which can be a pseudoknot or a simple hairpin positioned 5-8 nts downstream of the slippery sequence (34). The specific formulation of the slippery sequence is chosen to facilitate tRNA re-pairing to (near-)cognate codons after the shift (32). The downstream RNA secondary structures play a critical role in pausing ribosomes at the right position i.e. the XXY codon in the P-site and YYZ codon in the A-site to induce -1 PRF (35, 36). Although pausing is necessary, a biochemical study showed that pausing is not sufficient to induce -1 PRF (37), implying that the downstream secondary structures have an active role in this process, presumably by lowering the energy barrier for tRNA-mRNA un-pairing during translocation (38, 39). In a recent study using single-molecule optical tweezers the mechanical forces exerted by a single ribosome to unfold mRNA hairpins with different GC contents have been quantified (40). These data may help to shed light on the mechanical aspects of -1 PRF.

The diversity of -1 PRF-stimulating RNA motifs is remarkable and worthy of attention. Generally a pseudoknot is believed to be an efficient -1 PRF stimulator because of the extra stabilization from loop-stem interactions or other unknown factors that stabilize the pseudoknotted conformation at equilibrium at 37 ℃ (41). Simple hairpins, however, without complicated tertiary interactions as in pseudoknots are also genuine -1 PRF stimulators. Even antisense oligonucleotides that may form hairpin or pseudoknot-like structures have been reported to induce substantial -1 PRF. These elaborate frameshifting structures will be demonstrated and discussed below.

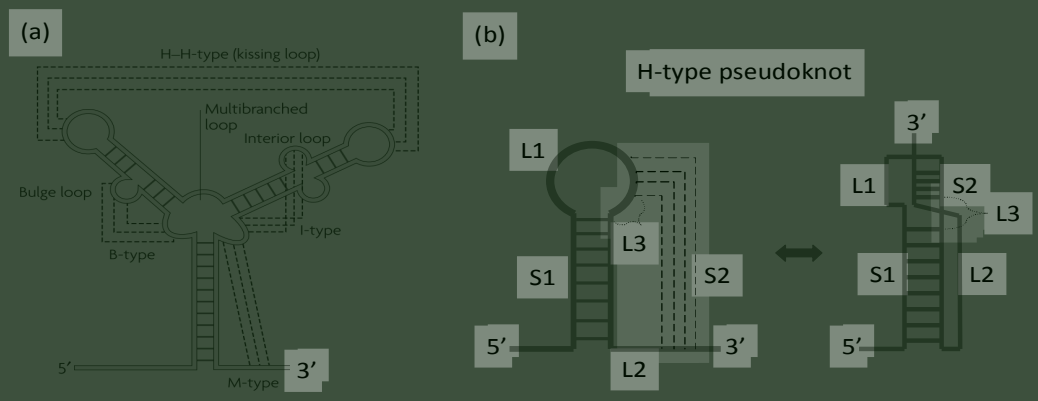

Figure 1. Various structures of RNA pseudoknots. (a) Different types of RNA pseudoknots (except H-type) are categorized by the motif that is responsible for the formulation of the second stem with the sequences outside the major stem-loop structure. (b) The representative structure of an H-type pseudoknot. The "S" denotes the stem region and the "L" indicates loop region. (adapted from Brierley *et al.*, 2007)

2. The structures of frameshifting pseudoknots

A pseudoknot, which was first discovered in Pleij's lab (42) almost 30 years ago, is defined as an RNA structure element formed upon standard base pairing of nucleotides of a loop region with residues outside the loop (43). Depending on the geometry of the loop, several types of pseudoknots, including H (hairpin), B (bulge), I (interior), or M (multibranched)-type, are recognized (Figure 1a) in various kinds of RNAs (44). The majority of pseudoknots that has been described to date are H-type pseudoknots which involve the apical loop of a hairpin; these will be referred to simply as pseudoknot in this chapter. A pseudoknot consists of two base-paired stem regions, S1 and S2, which are coaxially stacked and connected by two single-stranded loops, L1 and L2 (Figure 1b). L1 crosses the major groove of lower stem S2, while L2 crosses the minor groove of S1 (41). Some pseudoknots contain one or more unpaired nucleotides between the two stems and these nucleotides, referred to as L3, are either extruded from the junction of the two stems (45, 46) or intercalated between the two stems resulting in a specific bending (47).

Pseudoknots widely exist in RNA molecules including rRNA, mRNA, tRNA, transfer-messenger RNA (tmRNA), self-splicing RNA, and viral RNA (34, 44, 48, 49). Owing to their special 3D-structure, pseudoknots are often crucial elements in biological processes that are controlled by RNA structure. For example, riboswitches (50), telomerase (51), internal ribosome entry sites (IRES) (52–54), and several RNA-protein interactions (55) are dependent on pseudoknot formation for their function. Furthermore, pseudoknots play a key role in promoting recoding events. In this review, I will focus on the pseudoknots that induce efficient -1 PRF. The currently

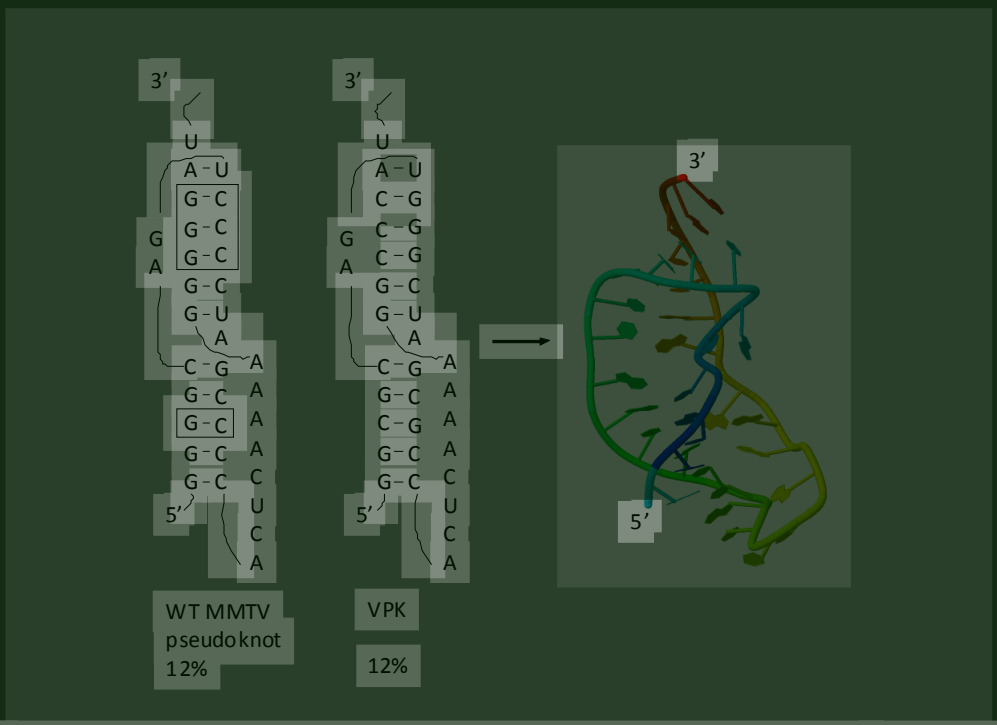

Figure 2. Structure representation of wt MMTV frameshifting pseudoknot and its derivative VPK solved by NMR spectroscopy (PDB 1RNK). The altered base pairs are boxed and the reported frameshifting efficiencies of both constructs are indicated.

available -1 PRF-inducing pseudoknot structures can be roughly divided into three groups. The first and second group are defined by the length of S1: (i) pseudoknots with S1 equal or smaller than 6 base pairs (bp), and (ii) those with S1 longer than 6 bp. The third group consists of pseudoknots with unusual structural features such as extra stems or loops. The differences of these signals between and within groups will be discussed in more detail below.

2.1 Group 1: pseudoknots with short S1

In this group there are three major types depending on certain specific structural features, and each has its representative pseudoknot: the *Mouse mammary tumor virus* (MMTV) *gag-pro* (56), the *Simian retrovirus type-1* (SRV-1) *gag-pro* (57), and plant luteoviral P1-P2 frameshifter pseudoknots (58). The MMTV *gag-pro* pseudoknot was the first -1 PRF signal whose solution structure was solved (59), and was also extensively studied by mutation analysis and structure probing (56, 60). Since then it has become a paradigm for -1 PRF stimulatory motifs. Note that the resolved structure (Figure 2) is a variant of wild-type (wt) MMTV pseudoknot called VPK with four G-C bps flipped to C-G bps while the frameshift-inducing ability remains unchanged (60). The analyzed structure reveals a 5 bp S1 crossed by L2 having 8 nts, while the 2

nts of L1 cross the deep groove of a 6 bp S2. The most interesting feature is an unpaired adenosine at the 3'-side of the helical junction of S1 and S2. This protruding nucleotide results in a pronounced bending about 60° from the vertical axis between two helices (59). Straightening of the pseudoknot by removal of the wedged adenosine decreases frameshifting efficiency dramatically (61–63). Further attempts to modify the direction of bending also resulted in inactive pseudoknots in -1 PRF. Therefore, the MMTV gag-pro represents a type of -1 PRF inducing pseudoknot that requires a specificly bent conformation as a frameshifter. Similar requirements were found for the *Feline immunodeficiency virus* (FIV) *gag-pol* (64) and the human paraneoplastic antigen *Ma3* gene frameshifter pseudoknots (29).

The representative of the second type in this group is the SRV-1 *gag-pro* pseudoknot (Figure 3). The dominant feature of this type is the coaxial stacking of S2 on top of S1. In the early studies of the SRV-1 pseudoknot, the presence of an adenosine kink at the junction of S1 and S2 was proposed, based on the observation that disruption of the putative A13-U29 (Figure 3, denoted as NMR SRV-1 pseudoknot) base pair at the junction had no effect on -1 PRF efficiency (65). However, two NMR studies have confirmed the A-U base pair by assignment of the imino proton of U29 (66, 67), which is also in agreement with the enzymatic probing results of the initial SRV-1 pseudoknot study (57). However, the solution structure did not answer the question of why A · A, A · G, or A · C mismatches at this position had no effect on frameshifting (60, 65). The confirmation of the A-U base pair at the junction further indicates that a bent conformation is dispensable for -1 PRF pseudoknots although a smaller bending allowing the single nucleotide of L1 to span S2 has been observed (67).

The identity of the single nucleotide of L1 was found to be unrelated to -1 PRF efficiency indicating this nucleotide is merely to function as a bridge between S1 and S2 and, at the same time, spans the major groove of S2 (68). However, the length and identity of L2 are highly relevant for the function of the SRV-1 pseudoknot. Although not exhaustively studied, the optimal length of L2 has been reported to be 8 to 10 nts, which is shorter than the wt L2 of 12 nts (68, 71). The sequence identity of L2 was initially thought to be less relevant since changing 10 out of 12 bases did not affect frameshifting efficiency (68). However, a recent functional study of the SRV-1 pseudoknot has shown that the identity of bases, especially those that are close to the junction, is indeed critical (69). A possible explanation for these contradictory findings is that the two nts proximal to the junction that are important for -1 PRF pseudoknot were maintained in the earlier study (68).

In addition to loops, a role for stems in -1 PRF has also been proposed for the SRV-1 pseudoknot. It was found that the calculated stability of S1 is not correlated to frameshifting efficiency but that the presence of G-C base pairs in the lower half of S1 is important; conversely, the thermodynamic stability of S2 was observed to correlate with frameshifting efficacy although no clear linear dependence was revealed. These results inspired the authors to propose that a certain threshold stability of the first few base pairs in S1 was important to stall ribosomes over the slip site, then the approaching ribosomes might be designated to alternative fates depending on the stability of S2 (68). A hybrid pseudoknot frameshifter (DH40) build up from S2 of a non-frameshifting pseudoknot from bacteriophage T2, and a coaxially stacked S1 of a frameshifting pseudoknot in the *gag-pro* junction of *Human endogenous retrovirus* (HERV)-K10 may support this idea. DH40, although preserving the structure of the T2 pseudoknot, induced identical levels of frameshifting as the wt HERV pseudoknot. NMR data showed a similar local structure at the junction of the stems in hybrid (active) and T2 pseudoknot (inactive), indicating that the relatively unstable S1 (two A-U base pairs in S1) of the T2 pseudoknot, may not exceed the threshold to fix ribosomes over the slippery sequence (70).

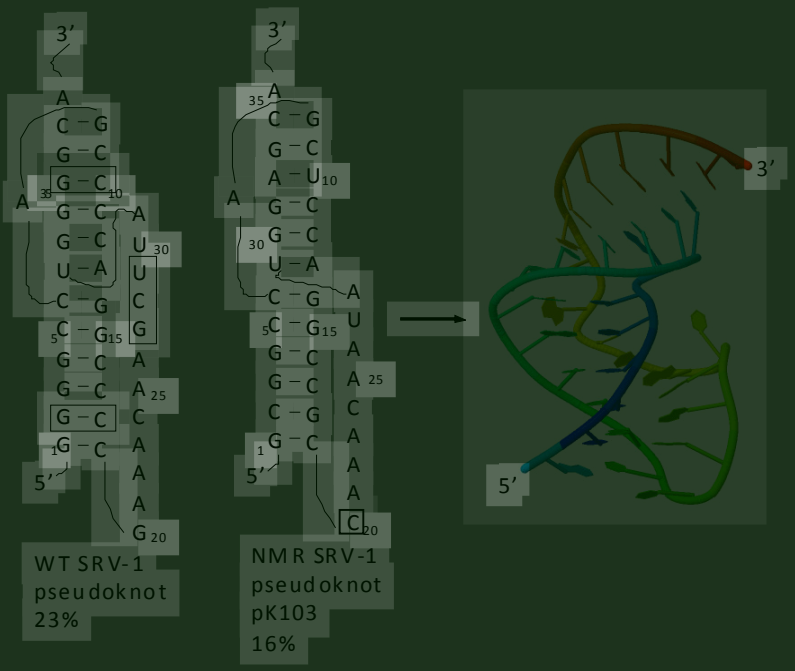

Figure 3. Structure representation of wt SRV-1 frameshifting pseudoknot and its derivative pk103 solved by NMR spectroscopy (PDB 1E95). The differences between wt and pk103 are indicated by boxes.

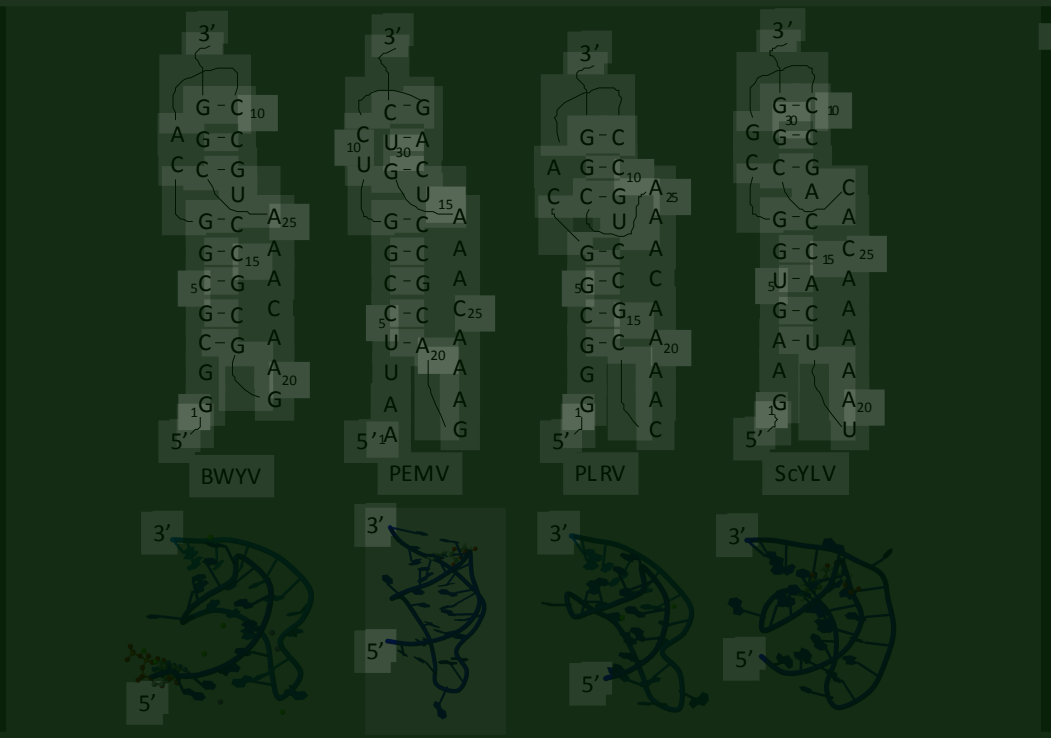

Figure 4. Structure representation of luteoviral frameshifting pseudoknots. The solved structures are also shown. PDB codes of BWYV, PEMV, PLRV, and ScYLV are 1L2X, 2RP1, 2A43, and 1YG4, respectively.

The third type in this group comprises the P1-P2 pseudoknots of plant luteoviruses (Figure 4). The representative pseudoknot is present at the overlapping P1-P2 genes of *Beet western yellow virus* (BWYV). This pseudoknot was initially proposed to consist of two coaxially stacked short stems (5 bps of S1 and 4 bps of S2) connected by a 2 nts L1 and a 6 nts L2 (34). In fact, after the crystal structure of the pseudoknot was obtained (71), a different picture emerged. The predicted U13-A25 base pair at the top of S2 does not exist but an unpaired U13 is present at the helical junction. Although similar to the MMTV *gag-pro* pseudoknot with non-coaxially stacking of S1 and S2, the distortion of S2, however, resulting from the short length of L1 and continuous stacking of L2 on A25 together with the bulged out U13 make the BWYV P1-P2 pseudoknot a distinct type of -1 PRF stimulating pseudoknot.

Another remarkable feature is the minor groove triplex between L2 and S1. A conserved 5'-AACAAA-3' sequence found in the 3'-end of L2 forms numerous non-canonical base-base or base-sugar hydrogen bonding interactions using their Watson-Crick edges in the minor groove of S1. This kind of S1-L2 interaction was first described for BWYV and later on shown to exist in other luteoviruses, including *Pea enation mosaic virus* (PEMV), and *Potato leaf roll virus* (PLRV) (58, 72–74) (Figure 4). It is noteworthy that the 3' adenine (the last nucleotide in L2) extensively

interacts with neighboring nucleotides through its Watson-Crick and Hoogsteen faces to stabilize the junction (74, 75). Interestingly, a highly similar L2 sequence 5'-AAACAAUA-3' is present in a non-related pseudoknot pk103, which is a modified version of wild–type SRV-1 *gag-pro* pseudoknot used for NMR studies (67). Several adenines of this L2 are involved in triplex formation with S1 like the luteovirus L2 sequences. However, a different structural detail is present: the N4 amino group of the cytidine in BWYV-type L2 forms a hydrogen bonding with the 2'OH of a G residue in S1 whereas the cytidine is bulged out from the L2 in the solution structure of pk103.

In *Sugar cane yellow leaf virus* (ScYLV) the C25 is bulged out as well (Figure 4) and the deletion mutant shows increased frameshift-indcucing activity (76). Mutational analyses have confirmed these findings from structural studies and shown the C is critical in luteoviral frameshifting pseudoknots (77), whereas the C in pk103 can be replaced by any other nucleotide without affecting or even partially increasing frameshifting efficiency (69). These results further demonstrate the diverse nature of frameshifting pseudoknots.

In addition to minor groove triples, a protonated cytidine in BWYV L1 forms a standard Hoogsteen base pair with the G-C in S2 and aligns in the major groove of S2. This major groove C^+ · G-C triple is conserved in all luteoviral pseudoknots, and shown to strongly enhance the pseudoknots stability (78, 79) and their frameshifting efficiency (76, 78). Although this is the only known group of natural -1 PRF stimulators showing this structural feature, the human telomerase pseudoknot hTPK-DU177 was recently found to be an efficient frameshifting stimulator whose activity is strongly correlated with the presence of major groove triples (80). These data may further improve the algorithm to propose more frameshifting related pseudoknot structures in the future.

The nature of life is the presence of exceptions. The pseudoknot in the P1-P2 junction of ScYLV, although still a luteovirus, reveals some structure variations (50, 82). For example, the 9 nts L2 of the ScYLV pseudoknot align well in the minor groove of S1 forming a triple helix and exhibit continuous base stacking, except for one cytidine which is extruded from the triplex whereas other luteoviral pseudoknots feature extruded nucleotide(s) proximal to the junction of S1 and L2 and continuous base stacking of the 3' side of L2. The most striking difference is the identity of the nucleotide of the L2 in the helical junction. In ScYLV, the N3 of cytidine (C27) at the 3'end of L2 forms a hydrogen bonding with the 2'OH of a cytidine paired with guanosine (C14-G7) while an adenosine is found at the relative position in BWYV, PLRV, and, PMEV to interact with 2'OH via N1 (48). An interesting study showed that the C27A mutant of ScYLV is almost inactive in frameshifting although both wt

and mutant pseudoknots adopt indistinguishable global structures (82), and further comparison showed that the structure of helical junction of the C27A mutant is superimposable on that of the BWYV pseudoknot. These data suggest that the "ground-state" structure does not directly correlate with frameshifting. Since the A25C mutation in the helical junction of the BWYV pseudoknot does improve frameshifting (83), it can be concluded that stability of the helical junction is disfavorable for the architecture in the C27A mutant (82). The exact details still need to be elucidated.

2.2 Group 2: pseudoknots with long S1

The frameshifting pseudoknots in the second group feature a longer S1 compared to those of the first group. Most notably, the sequence identity of L2 is independent of frameshifting efficiency (32), indicating that no L2-S1 triple helix is needed to stabilize these pseudoknot structures, although a recent study of mammalian coronavirus frameshifting pseudoknots demonstrated opposite results (84). Due to the absence of a three-dimensional structure either in crystal or solution, the precise role of L2 in long S1 pseudoknots is still a matter of debate.

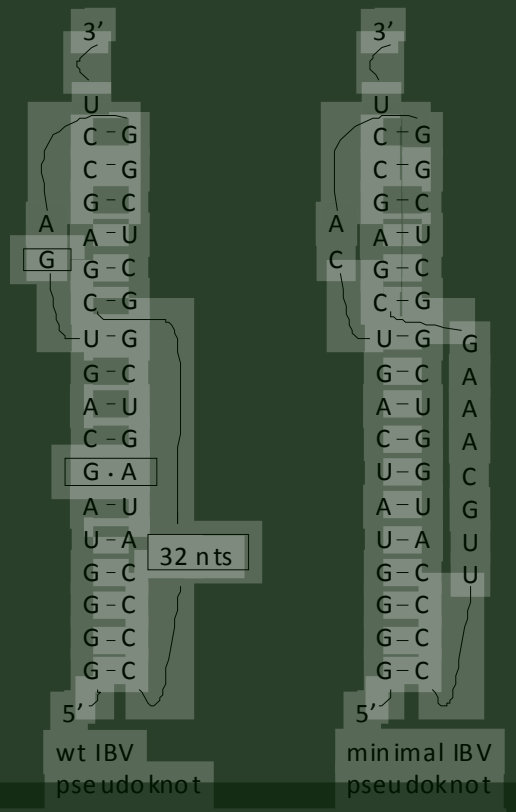

Figure 5. Structure representation of wt IBV pseudoknot and its derived minimal IBV pseudoknot, the wt in nowadays. The differences are boxed.

The most representative pseudoknot in this group is the frameshift-stimulatory signal present at the 1a-1b overlap of avian coronavirus IBV (85). Although discovered over 20 years ago, the three-dimensional structure is still unknown, and the detailed information of this frameshifting pseudoknot comes from mutational studies and probing analysis mainly contributed by Brierley's group (86). The topology of the wt IBV frameshifting pseudoknot is an 11 bp S1 and 6 bp S2, linked by a 2 nts L1 and an L2 of 32 nts without apparent structure (Figure 5) (85). The IBV frameshifting signal is located 6 nts downstream of a U_UU.A_AA.C slippery sequence. In vitro frameshifting assays have shown that an 8 nts loop can effectively substitute the wild type 32 nts L2. This modified pseudoknot, named minimal IBV pseudoknot is the "current" wt IBV pseudoknot (Figure 5) (87).

This functional variant with much shorter L2 may indicate that a certain length of L2 is simply needed to cross the 11 bps in S1 (88). For IBV it has been shown that the length rather than the thermodynamic stability of S1 is critical for frameshift activity (89). Removal of a single bp in S1 reduces frameshifting already 7 fold, removal of 2 bps from S1 almost abolishes its activity, even though thermodynamic stability and overall structure, as determined by probing, are similar to the wt pseudoknot. On the other hand, pseudoknots having longer S1 stems (12-14 bp) were fully functional in frameshifting (89).

The relatively weak G-U base pair at the top of S1 was examined to see if the IBV pseudoknot adopts an intercalated structure like the MMTV or luteovirus frameshifting signals. Replacing G-U with the more stable G-C or C-G base pairs promotes frameshifting efficiency at slightly higher level (87, 89). Combined with structural probing data (89) it seems unlikely that there is a kink nucleotide in the helical junction. However, an unpaired nucleotide is of great importance to a shorter S1 (6 bp) variant of the IBV pseudoknot. Similar to the MMTV pseudoknot (56, 61), an inactive IBV-like pseudoknot was converted into an efficient frameshifting stimulator, named pKA-A, when an unpaired adenosine was inserted into the helical junction, meanwhile the last nucleotide of L2 was switched from G to A (90). Inverting the fourth, C-G, and fifth, G-C, bps of pKA-A S1 decreased frameshifting about 3.5-fold, indicating there are specific S1-L2 interactions like those observed in group I introns (91) and the *turnip yellow mosaic virus* (TYMV) tRNA-like pseudoknot (92). However, the requirement for this interaction is bypassed when the length of L2 is increased to 14 nts. High-resolution structures may help to uncover the relation between L2 length and sequence identity of S1 (86).

Further studies have shown related frameshifting pseudoknots within the *1a-1b* overlapping region in other coronaviruses genomes, including murine hepatitis virus (MHV) (93), human coronavirus (HCoV)-229E (94), and the recently identified SARS-coronavirus, the causative of agent severe acute respiratory syndrome (SARS), (95). Extensive mutational studies, RNA structure probing analysis, and preliminary NMR data have shown that the frameshifting signal of SARS-CoV, located 6 nts downstream of an UUUAAAC slip site, adopts an H-type pseudoknot possessing an additional hairpin called S3 or SL1 within L2 (Figure 6) (96–99).

Similar to other frameshifting pseudoknots, disruption of base pairs in either S1 or S2 severely reduces frameshifting efficiency further confirming the pseudoknot conformation. However, disruption or deletion of S3 in the L2 region has no dramatic effect on stimulating frameshifting both *in vitro* and in cultured cells (97–99). It was, therefore, proposed that the necessity of S3 is not for efficient ribosomal frameshifting

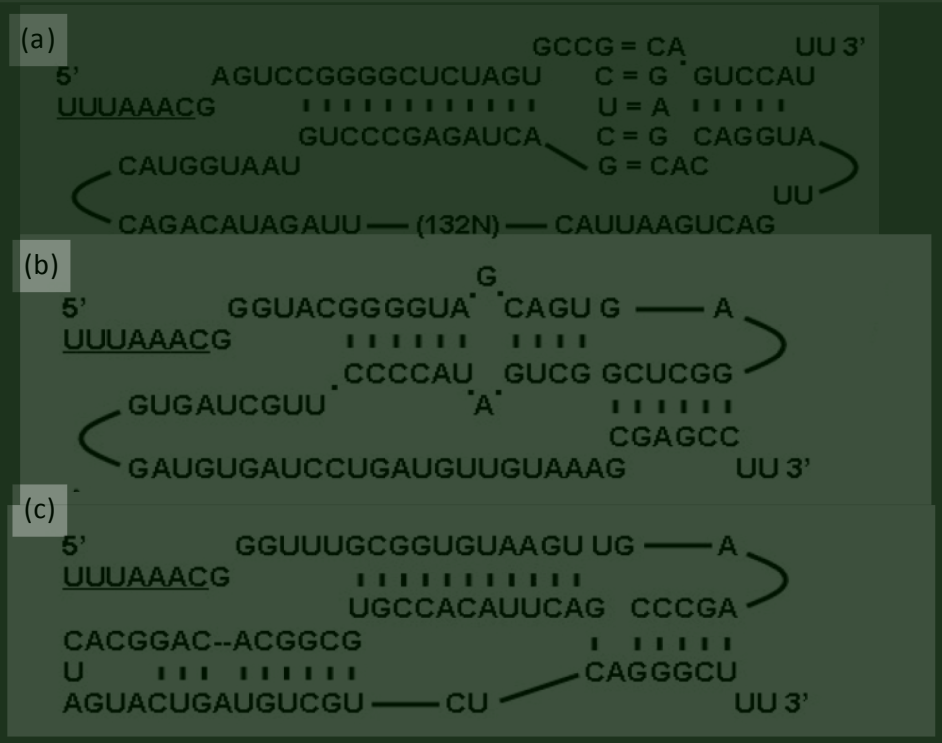

Figure 6. Structure representation of the representative of frameshifting pseudoknots in three groups of coronavirus. (a) The frameshifting pseudoknot of HCoV-299 belonging to group 1 coronavirus. (b) The frameshifting pseudoknot of IBV belonging to group 2 coronavirus. (c) The frameshifting pseudoknot of SARS-CoV belonging to group 3 coronavirus. (taken from Plant *et al.*, 2008)

but for global folding of the pseudoknot (97) or for functional switching between transcription and translation by RNA remodeling as proposed for another (+) strand RNA virus (98). The last assumption, although elegant and promising, seems controversial since the S3 is not conserved in all three groups of coronaviruses. In all group 2 coronaviruses, including SARS-CoV and MHV, the S3 motif resided in L2 can be identified in their frameshifting pseudoknots (Figure 6). However, in group 3 coronaviruses such as IBV the L2 seems to be a single-stranded loop. In addition, the frameshifting pseudoknot of group 1 coronaviruses, like HCoV-229E, forms a more "elaborated" structure as the S2 is formed by kissing loops connected by a long, 150 nts, L2 without apparent secondary structure (Figure 6) (94, 100).

A diversity of frameshifting stimulatory structures has recently been defined in Alphaviruses to stimulate production of transframe (TF) protein which overlaps the 6K ORF (101). One of these stimulatory structures is a pseudoknot, found in *Middelburg virus* (MIDV), featuring (Figure 7): (i) an unstable 3 bp lower S1 and high GC content 7 bp upper S1 interrupted by an A · G mismatch; (ii) a 7 bp S2; (iii) 3

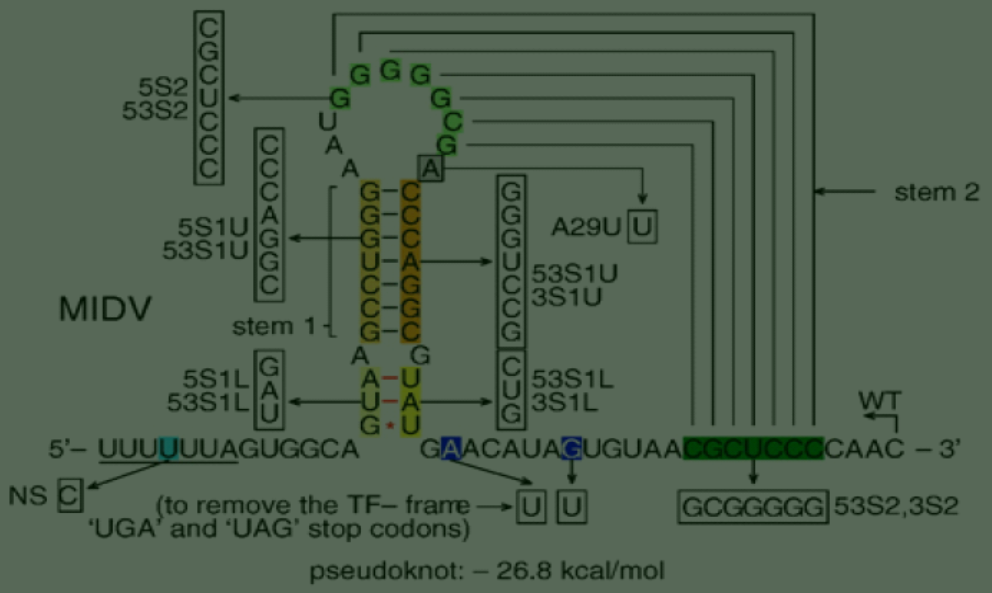

Figure 7. Structure representation of MIDV frameshifting pseudoknot. The dark and light green shaded sequences are base-paired to form S2. Orange shaded region indicates upper S1 while yellow shaded region indicates unstable lower S1. Boxed sequences are the mutations made by Chung and colleagues. (Taken from Chung *et al.*, 2010)

nt L1, 13 nt L2, and a single adenosine in between the two stems, reminiscent of the MMTV frameshifting pseudoknot. Interestingly, destabilizing the lower part of S1 resulted in comparable frameshifting efficiency whereas stabilizing it decreased frameshifting 4-fold (102). This is similar to the HIV-1 frameshifting hairpin that requires a lower stem to position the translating ribosomes (see below). Modifying the A between the stems to U has no significant effect suggesting that this nucleotide is only necessary to span the major groove. Intriguingly, the first 6 nt of the spacer together with the slippery sequence (U.UU_U.UU_A) are somehow capable of inducing 5% of frameshifting. In some Alfaviruses frameshifting seems to occur without apparent stimulatory structures (102). How this is achieved is not yet known.

2.3 Group 3: odd pseudoknots

An example of a B-type, bulge type, pseudoknot is found in the overlapping region of ORF1 and ORF 2 of *Barley yellow dwarf virus* (BYDV), an RNA plant virus belonging to the genus Luteovirus of the Tombusviridae. In this pseudoknot 6 nts that are located four thousand nucleotides more downstream can base pair to a bulge loop of the hairpin structure (Figure 8) adjacent to the GGGUUUU slippery sequence in the ORF1/2 overlap (103, 104). This long-distance interaction is not only conserved in a BYDV-like virus, *Soybean dwarf virus* (SbDV) (Figure 8) (104) but has also recently been discovered in *Red clover necrotic mosaic virus* (RCNMV), a member of

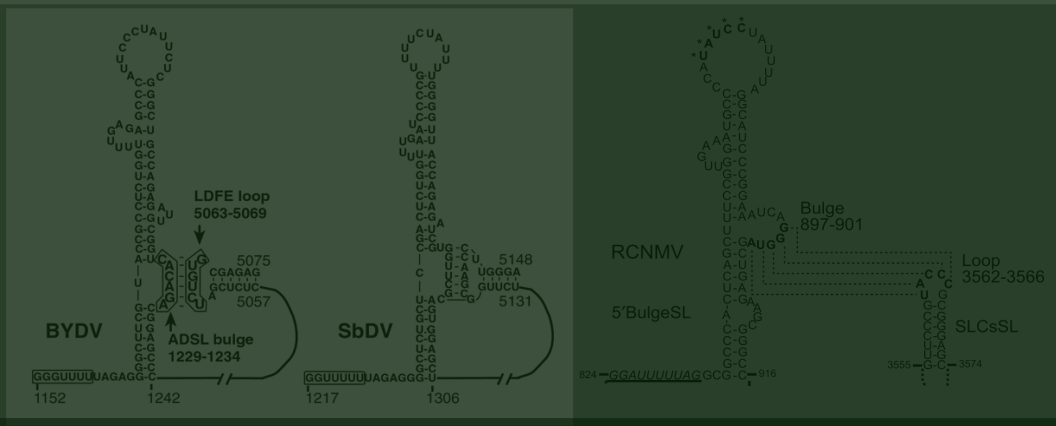

Figure 8. Three representative bulge-apical loop frameshifting pseudoknots in plant viruses. The bulge residing in main stem-loop structure base pairs with the apical loop of another stem-loop in 3'UTR thousands nucleotides downstream. The numbers indicate the nucleotide positions in each RNA virus genome (figures of BYDV and SbDV are taken from Barry *et al.*, 2002; figure of RCNMV is taken from Tajima *et al.*, 2011).

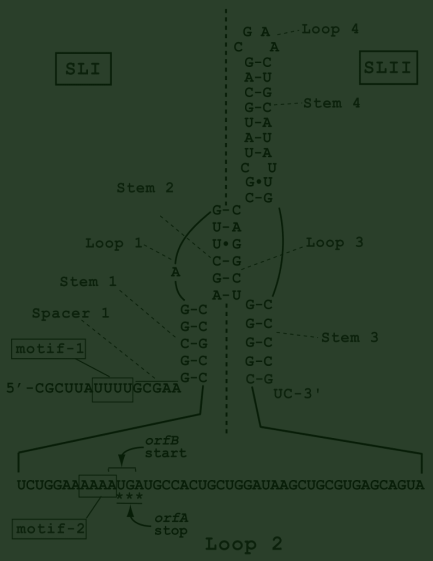

Figure 9. Structure representation of apical loop-internal loop frameshifting pseudoknot. The apical loop from stem-loop structure 1 (SLI) forms a 6 bp stem with the internal loop of the 45 nts downstream stem-loop 2 (SLII) to induce frameshifting over the UUUU (motif-1) slippery sequence in IS*3411*. (taken from Mazauric *et al*., 2008)

the genus Dianthovirus, also of the Tombusviridae (Figure 8) (105). This and anotherlong-distance interaction that stimulates translation initiation of BYDV are proposed to be involved in regulation of competition between translation andtranscription, an important issue for all (+) strand RNA viruses (104).

A novel type of frameshifting pseudoknot of which the S2 is formed by base pairing of the apical loop and internal loop of two stem-loop structures was identified by Mazauric *et. al.* in IS*3411*, a transposon of the IS*51* group of insertion sequences in eubacteria (Figure 9) (106). It was shown that the stability of the structure corrrelated with frameshifting efficiency and transposition, indicating that this new type of pseudoknot is of biological relevance. Interestingly, when the second hairpin (Figure 9, SLII) was cloned into the anticodon arm of a tRNA and expressed together with the remainder

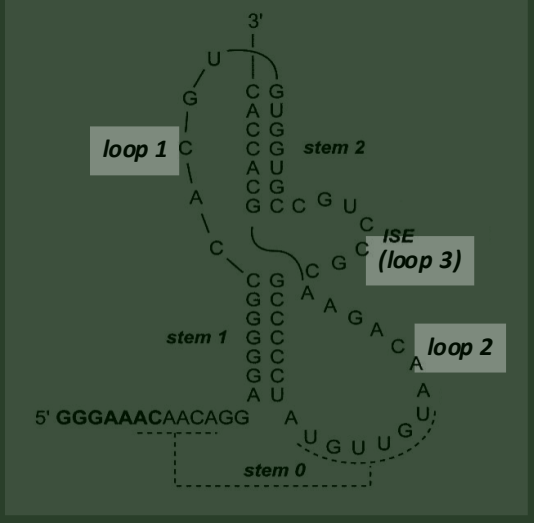

Figure 10. Structure representation of VMV frameshifting pseudoknot. The slippery sequence is shown in bold. A possible interaction of spacer with loop 2 is indicated by dashed line (stem 0). The relatively large 7 nt loop3, interstem element (ISE) is the unique feature of this pseudoknot. (adapted from Pennell *et al.*, 2008)

of the pseudoknot located on the mRNA, frameshifting was observed only when the 6 bp in stem 2 could form.

The frameshifting stimulator of the ovine lentivirus Visna-Maedi retrovirus (VMV) was confirmed to be a pseudoknot instead of a simple stem-loop (Figure 10) (107). Two interesting structural features were identified. First, a 5 nt L1, which is generally 1 or 2 nt in reported frameshifting pseudoknots to connect S1 and S2 is present. There are two cytidines in L1 that have potential to form $C^+ \cdot G$-C triples with S2. However, only one deletion mutant in which the last three nts were removed was examined and it was shown to be inactive in frameshifting, implying that L1 is not only for bridging but unknown interactions to stabilize VMV pseudoknot. Furthermore, a relatively large 7 nt L3 termed interstem element (ISE) is present in between S1 and S2, and this GC rich fragment was also shown to be crucial in inducing frameshifting. Either shortening or lengthing ISE dramatically reduced frameshifting efficiency. Changing the ISE sequence to alternate purine/pyrimidine bases while maintaning the stem length still resulted in a 5-fold decrease in frameshifting efficiency, indicating that

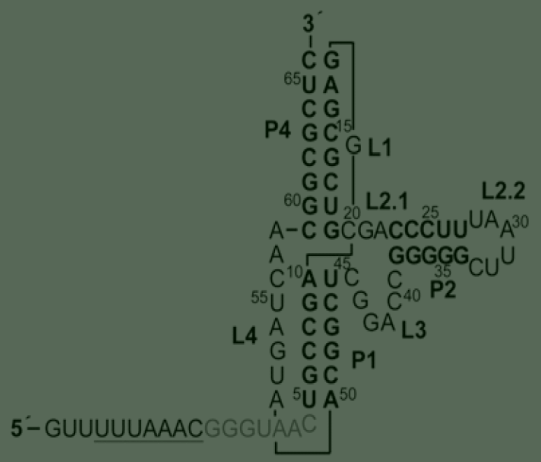

Figure 11. Structure representation of three-stemmed pseudoknot aptamer of SAH riboswitch located 7 nt dowstream of UUUAAAC slippery sequence. The elements of this pseudoknot are indicated. A large and structured L2 (the L3 in this thesis) is present in between two stems. (taken from Chou *et al.*, 2010)

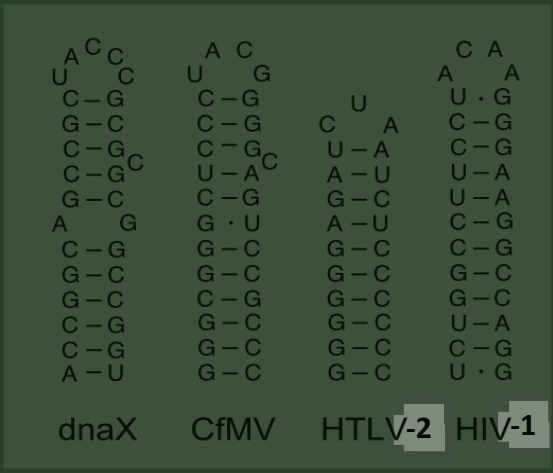

Figure 12. Structure representation of four different frameshift-inducing hairpins. (adapted from Yu *et al.*, 2011)

both the identity and the length of the sequence are important.

An interesting example of ametabolite-responsive frameshifting signal was recently reported. The three-stemmed pseudoknot (Figure 11) of an S-adenosylhomocysteine (SAH) riboswitch can specificly respond to ligand concentrations to induce different levels of frameshifting in *vitro* and in *vivo* (108). The ligand has been shown to stabilize the junctions between the different stems, which are dynamic in the absence of SAH. Although this is not a natural frameshifting pseudoknot, the finding of inducible frameshifting suggests that cellular factors may regulate -1 PRF through a mechanism that so far has only been found in +1 PRF (8).

3. Stem-loop structures

It has long been considered that a hairpin stimulates frameshifting to a lesser extent than a pseudoknot, although both RNA structures can pause ribosomes to a similar degree (109–111). Certain exceptions, however, were found upon testing identical frameshifting constructs in *E. coli* (112) or a modified wheat germ (WG) *in vitro* translation system (113). Nevertheless, there are several frameshifting inducing stem-loop structures identified, including *gag-pol* junction of lentiviruses HIV-1 and *Simian immunodeficiency virus* (SIV)/HIV-2 (114–117), the *gag-pro* junction of *Human T-cell leukemia virus type II* (HTLV-2) (118, 119), the junction between ORF 2a and ORF 2b of *Cocksfoot mottle virus* (CfMV) (120–122), and in decoding two *dnaX* products gamma (γ) and tau (τ), two subunits of DNA polymerase III of *E. coli* (123, 124). Decoding of *dnaX* is an unusual type of frameshifting in the sense that the frameshift leads to a protein γ, which is shorter than the non-shifted protein, τ, while in other cases of programmed frameshifting it is the opposite. The frameshifting signals consist of (i) a SD-like sequence upstream of highly slippery sequence AAAAAAG, reminiscent of +1 frameshifting of RF2 in *E coli* (11) and probably responsible to further stall translating ribosomes over slippery sequence; (ii) a downstream stem-loop structure. All of them are necessary to synthesize γ and τ in an 1:1 ratio. The chemical probing analysis showed that the frameshift-inducing

hairpin (Figure 12) features an 11 bp stem with a A · G mismatch in the middle, a C bulge at the 3' side of the stem located 3 bp from the closing base pair (cbp), and a UACCC pentaloop (124). Mutational analysis *in vivo* demonstrated that removing the C bulge, restoring A · G to C-G, or adding a G to pair with the bulged C, all lead to higher frameshifting efficiency. Combined with results of other mutants, the authors concluded that the calculated stability of the stem-loop structure is positively correlated with frameshifting efficiency with and without SD-like stimulatory sequence. An independent study of assaying frameshifing efficiency of six HIV-1 hairpin mutants in yeast and cultured cells reached the same conclusion although with limited number of constructs (125).

The viral protease VPg and RNA-dependent RNA polymerase (RdRp) of the plant virus CfMV are expressed from two overlapping ORFs by means of -1 PRF (126). The stimulatory signal is characterized as a 12 bp stem with a C bulge at the 3' side positioned 3 bp away from the stable UACG tetraloop (Figure 12) (120). The location of the bulge is similar as in the frameshifting hairpin of *dnaX*, but whereas adding an complementary G increased frameshifting efficiency in *dnaX* construct (124) it had no effect on frameshifting in the CfMV construct (122) assayed in an WG *in vitro* translation system. Enlarging the loops of the *dnaX* and CfMV hairpins by 6 and 3 nts, respectively, slightly elevated their frameshifting efficiency. Remarkably, deletion of the C bulge, although not affecting frameshifting efficiency *in vitro*, proved to be deleterious to CfMV infection activity whereas the 3 nts enlarged-loop mutant kept a wt level of infectivity (122), suggesting that the specific RNA structure may be critical in physiological function of virus and can not be simply concluded by frameshifting efficiency. On the other hand, the effect of a modified RdRp peptide sequence by the C deletion needs to be taken into account. Moreover, co-expression of P27 viral protease but not replicase reduced production of the downstream reporter when the minimal frameshifting signal was present (127). This phenomenon is similar to the feedback regulation of antizyme synthesis (21), RF2 (11), and the eRF1 interaction with reverse transcriptase of *Moloney murine leukemia virus* (MuLV) (128), but the mechanism in CfMV still needs to be investigated.

The frameshift-inducing element in HTLV-2 is a 10 bp perfect stem capped by a CUA triloop (Figure 12) (119). On the basis of an extensive mutational analysis by shuffling of HIV-1 and HTLV-2 frameshifting RNA elements in a background of HIV-1 or HTLV-2 sequences, it was proposed that the frameshifting efficiency is not only determined by slippery sequences and stimulatory secondary structures but also largely affected by sequences upstream of slip site and the sequence of the spacer

region (119). However, closer examination of the correlation between frameshifting efficiency and the identity of the first nucleotide of the spacer shows no similar trend as proposed by Fayet's lab that the strong stacking of purine may stabilize the codon-anticodon interaction at the A site of slippery sequence thereby reducing frameshifting efficiency (129).

The discovery that -1 PRF is responsible for gag-pol polyprotein expression in HIV-1 was made more than 20 years ago (33) but the exact nature of the stimulatory structure has long been debated. Through extensive mutational and structure probing studies, combined with sequence alignments and NMR structure analysis (114–117, 130), the frameshift stimulator of HIV-1 is generally believed to be a 11 bp stem with a highly ordered ACAA tetra loop rather than a pseudoknot structure (Figure 12) (131, 132). An additional 8 bp unstable lower stem was later proposed to contribute to the frameshift efficiency (116). Considering that the ribosome has to be positioned over the slippery sequence when stalled by the hairpin, the lower stem should be melted during -1 PRF. Hence, the exact function of the lower stem is unknown. It was proposed that the lower stem acts as a "positioning element" to allow the upper 11 bp hairpin to pause ribosomes which in turn mediates translocation perturbations via an unknown mechanism (116). It is well known that subtle modulations of Gag/Gag-Pol ratio have profound negative effects on HIV infection activity (133, 134). Hence, it has been proposed that the finding of either cellular proteins (135, 136) or small molecules (137, 138) that may interact with the HIV frameshifting hairpin and affect its frameshifting efficiency, have the potential to become anti-HIV drugs.

HIV-2 and SIV, belonging to the genus lentiviruses like HIV-1, have nearly identical frameshifting stimulatory structures but somewhat distinct from the HIV-1 frameshifting stem-loop (139). The major difference is the 12 nts loop of HIV-2/SIV, which has been proposed to incorporate a sheared G-A base pair, a cross-strand adenosine stacking, two G-C base pairs, and a novel CYC (Y = C in SIV, Y = U in HIV-2) triloop sequence. The spacer between slip site and "main" frameshifting hairpin comprises a C : C mismatch, a 4 bp helical stem, and 4 (SIV) or 5 nts (HIV-2) single stranded region making it one (SIV) or two (HIV-2) nucleotides longer than the spacer of HIV-1. Noticeably, the stem length of SIV/HIV-2 and HIV-1 is 11 bp which is similar to the S1 of the IBV frameshifting pseudoknot. Since a full helical turn A-form RNA duplex is 11 bp, it may imply a similar mechanism to stimulate frameshifting for these RNA structures (41, 48). Although it was suggested that SIV/HIV-2 frameshifting signal is a hairpin, extending the signal by another 12 nts increased frameshifting from 8.3 to 12.2% (Figure 13). Interestingly, this extended

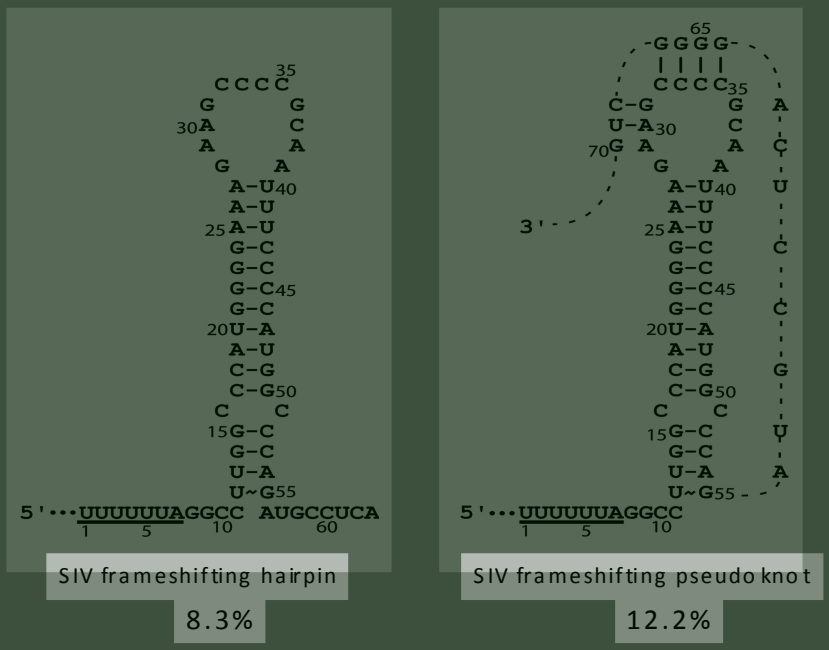

Figure 13. Structure representation of predicted SIV frameshifting hairpin and frameshifting pseudoknot. The reported frameshifting efficiencies *in vitro* are indicated. (adapted from Marcheschi *et al.*, 2007)

sequence can form a pseudoknot by base pairing with the 5'-AGCCCC- 3' sequence in the loop. This pseudoknot is conserved in all published strains (Olsthoorn, personal communication). So, similar to the HIV-1 group O retroviruses that make use of a pseudoknot instead of a simple stem-loop structure to regulate expression (140) the signal in SIV and HIV-2 retroviruses may be a pseudoknot as well. Why Butcher's lab has chosen to solve the structure of the less relevant hairpin structure remains unclear.

4. Antisense oligonucleotides (AONs)

Apart from natural examples of frameshifting structures, a novel finding has been the demonstration that synthetic AONs, annealed 3' of the slippery sequence and thereby mimicking a hairpin structure, are able to stimulate frameshifting *in vitro* (141, 142) and *in vivo* (143). In addition, AONs can also simulate triple helix (80) or kissing loop structures (106) to promote -1 PRF. These interesting results suggest that AONs act as physical barriers to stall ribosomes to stimulate ribosomal frameshifting and therefore are useful to dissect the mechanism of -1 PRF. Moreover, the great flexibility of AONs may have potential to treat frameshifting diseases.

Conclusion

A wide variety of structures are able to induce ribosomal frameshifting. Their

efficiency depends much on their thermodynamic stability but additonally kinetic and mechanical aspects should be considered. As a rule of thumb it can be postulated that the smaller the structures the more additional interactions i.e. base triples and quadruples they need to withstand the ribosomal helicase. The pseudoknot may be a perfect platform to bring together such interactions. Whether these structures are actively involved in the recoding event or merely a physical barrier that increases the time for tRNAs to repair remains a matter of debate.

Reference

1. Baranov,P.V., Gesteland,R.F. and Atkins,J.F. (2002) Recoding: translational bifurcations in gene expression. *Gene*, **286**, 187-201.

2. Gesteland,R.F., Weiss,R.B. and Atkins,J.F. (1992) Recoding: reprogrammed genetic decoding. *Science*, **257**, 1640-1641.

3. Namy,O., Hatin,I. and Rousset,J.-P. (2001) Impact of the six nucleotides downstream of the stop codon on translation termination. *EMBO Rep.*, **2**, 787-793.

4. Namy,O., Duchateau-Nguyen,G., Hatin,I., Hermann-Le Denmat,S., Termier,M. and Rousset,J.-P. (2003) Identification of stop codon readthrough genes in Saccharomyces cerevisiae. *Nucleic Acids Res.*, **31**, 2289-2296.

5. Bidou,L., Rousset,J.-P. and Namy,O. (2010) Translational errors: from yeast to new therapeutic targets. *FEMS Yeast Res.*, **10**, 1070-1082.

6. Hatfield,D.L. and Gladyshev,V.N. (2002) How selenium has altered our understanding of the genetic code. *Mol. Cell Biol.*, **22**, 3565-3576.

7. Howard,M.T., Aggarwal,G., Anderson,C.B., Khatri,S., Flanigan,K.M. and Atkins,J.F. (2005) Recoding elements located adjacent to a subset of eukaryal selenocysteine-specifying UGA codons. *EMBO J.*, **24**, 1596-1607.

8. Namy,O., Rousset,J.P., Napthine,S. and Brierley,I. (2004) Reprogrammed genetic decoding in cellular gene expression. *Mol. Cell*, **13**, 157-168.

9. Xu,J., Hendrix,R.W. and Duda,R.L. (2004) Conserved translational frameshift in dsDNA bacteriophage tail assembly genes. *Mol. Cell*, **16**, 11-21.

10. Baranov,P.V., Gesteland,R.F. and Atkins,J.F. (2004) P-site tRNA is a crucial

initiator of ribosomal frameshifting. *RNA*, **10**, 221-230.

11. Márquez,V., Wilson,D.N., Tate,W.P., Triana-Alonso,F. and Nierhaus,K.H. (2004) Maintaining the Ribosomal Reading Frame:: The Influence of the E Site during Translational Regulation of Release Factor 2. *Cell*, **118**, 45 – 55.

12. Devaraj,A. and Fredrick,K. (2010) Short spacing between the Shine-Dalgarno sequence and P codon destabilizes codon-anticodon pairing in the P site to promote +1 programmed frameshifting. *Mol. Microbiol.*, **78**, 1500-1509.

13. Curran,J.F. (1993) Analysis of effects of tRNA:message stability on frameshift frequency at the Escherichia coli RF2 programmed frameshift site. *Nucleic Acids Res.*, **21**, 1837-1843.

14. Adamski,F.M., Donly,B.C. and Tate,W.P. (1993) Competition between frameshifting, termination and suppression at the frameshift site in the Escherichia coli release factor-2 mRNA. *Nucleic Acids Res.*, **21**, 5074-5078.

15. Mansell,J.B., Guévremont,D., Poole,E.S. and Tate,W.P. (2001) A dynamic competition between release factor 2 and the tRNA(Sec) decoding UGA at the recoding site of Escherichia coli formate dehydrogenase H. *EMBO J.*, **20**, 7284-7293.

16. Belcourt,M.F. and Farabaugh,P.J. (1990) Ribosomal frameshifting in the yeast retrotransposon Ty: tRNAs induce slippage on a 7 nucleotide minimal site. *Cell*, **62**, 339-352.

17. Farabaugh,P.J., Zhao,H. and Vimaladithan,A. (1993) A novel programed frameshift expresses the POL3 gene of retrotransposon Ty3 of yeast: frameshifting without tRNA slippage. *Cell*, **74**, 93-103.

18. Guarraia,C., Norris,L., Raman,A. and Farabaugh,P.J. (2007) Saturation mutagenesis of a +1 programmed frameshift-inducing mRNA sequence derived from a yeast retrotransposon. *RNA*, **13**, 1940-1947.

19. Ivanov,I.P. and Atkins,J.F. (2007) Ribosomal frameshifting in decoding antizyme mRNAs from yeast and protists to humans: close to 300 cases reveal remarkable diversity despite underlying conservation. *Nucleic Acids Res.*, **35**, 1842-1858.

20. Petros,L.M., Howard,M.T., Gesteland,R.F. and Atkins,J.F. (2005) Polyamine sensing during antizyme mRNA programmed frameshifting. *Biochem. Biophys.*

Res. Commun., **338**, 1478-1489.

21. Matsufuji,S., Matsufuji,T., Miyazaki,Y., Murakami,Y., Atkins,J.F., Gesteland,R.F. and Hayashi,S. (1995) Autoregulatory frameshifting in decoding mammalian ornithine decarboxylase antizyme. *Cell*, **80**, 51-60.

22. Ivanov,I.P., Anderson,C.B., Gesteland,R.F. and Atkins,J.F. (2004) Identification of a new antizyme mRNA +1 frameshifting stimulatory pseudoknot in a subset of diverse invertebrates and its apparent absence in intermediate species. *J. Mol. Biol.*, **339**, 495-504.

23. Namy,O., Galopier,A., Martini,C., Matsufuji,S., Fabret,C. and Rousset,J.-P. (2008) Epigenetic control of polyamines by the prion [PSI+]. *Nat. Cell Biol.*, **10**, 1069-1075.

24. Park,H.J., Park,S.J., Oh,D.-B., Lee,S. and Kim,Y.-G. (2009) Increased -1 ribosomal frameshifting efficiency by yeast prion-like phenotype [PSI+]. *FEBS Lett.*, **583**, 665-669.

25. Jacks,T. and Varmus,H.E. (1985) Expression of the Rous sarcoma virus pol gene by ribosomal frameshifting. *Science*, **230**, 1237-1242.

26. Baranov,P.V., Fayet,O., Hendrix,R.W. and Atkins,J.F. (2006) Recoding in bacteriophages and bacterial IS elements. *Trends in Genetics*, **22**, 174-181.

27. Farabaugh,P.J. (1996) Programmed translational frameshifting. *Microbiol. Rev.*, **60**, 103-34.

28. Larsen,B., Gesteland,R.F. and Atkins,J.F. (1997) Structural probing and mutagenic analysis of the stem-loop required for Escherichia coli dnaX ribosomal frameshifting: programmed efficiency of 50%. *J. Mol. Biol.*, **271**, 47-60.

29. Wills,N.M. (2006) A Functional -1 Ribosomal Frameshift Signal in the Human Paraneoplastic Ma3 Gene. *J. Biol. Chem.*, **281**, 7082-7088.

30. Manktelow,E., Shigemoto,K. and Brierley,I. (2005) Characterization of the frameshift signal of Edr, a mammalian example of programmed- 1 ribosomal frameshifting. *Nucleic Acids Res.*, **33**, 1553-1563.

31. Clark,M.B., Janicke,M., Gottesbuhren,U., Kleffmann,T., Legge,M., Poole,E.S. and Tate,W.P. (2007) Mammalian Gene PEG10 Expresses Two Reading

Frames by High Efficiency -1 Frameshifting in Embryonic-associated Tissues. *J. Biol. Chem.*, **282**, 37359-37369.

32. Brierley,I., Jenner,A.J. and Inglis,S.C. (1992) Mutational analysis of the "slippery-sequence" component of a coronavirus ribosomal frameshifting signal. *J. Mol. Biol.*, **227**, 463-479.

33. Jacks,T., Power,M.D., Masiarz,F.R., Luciw,P.A., Barr,P.J. and Varmus,H.E. (1988) Characterization of ribosomal frameshifting in HIV-1 gag-pol expression. *Nature*, **331**, 280-283.

34. ten Dam,E.B., Pleij,C.W. and Bosch,L. (1990) RNA pseudoknots: translational frameshifting and readthrough on viral RNAs. *Virus Genes*, **4**, 121-136.

35. Tu,C., Tzeng,T.H. and Bruenn,J.A. (1992) Ribosomal movement impeded at a pseudoknot required for frameshifting. *Proc. Natl. Acad. Sci. U.S.A.*, **89**, 8636-8640.

36. Lopinski,J.D., Dinman,J.D. and Bruenn,J.A. (2000) Kinetics of ribosomal pausing during programmed -1 translational frameshifting. *Mol. Cell. Biol.*, **20**, 1095-1103.

37. Kontos,H., Napthine,S. and Brierley,I. (2001) Ribosomal pausing at a frameshifter RNA pseudoknot is sensitive to reading phase but shows little correlation with frameshift efficiency. *Mol. Cell. Biol.*, **21**, 8657-8670.

38. Namy,O., Moran,S.J., Stuart,D.I., Gilbert,R.J.C. and Brierley,I. (2006) A mechanical explanation of RNA pseudoknot function in programmed ribosomal frameshifting. *Nature*, **441**, 244-247.

39. Cornish,P.V., Ermolenko,D.N., Noller,H.F. and Ha,T. (2008) Spontaneous intersubunit rotation in single ribosomes. *Mol. Cell*, **30**, 578-588.

40. Qu,X., Wen,J.-D., Lancaster,L., Noller,H.F., Bustamante,C. and Tinoco,I.,Jr (2011) The ribosome uses two active mechanisms to unwind messenger RNA during translation. *Nature*, **475**, 118-121.

41. Giedroc,D.P., Theimer,C.A. and Nixon,P.L. (2000) Structure, stability and function of RNA pseudoknots involved in stimulating ribosomal frameshifting1. *J. Mol. Biol.*, **298**, 167-185.

42. Rietveld,K., Van Poelgeest,R., Pleij,C.W., Van Boom,J.H. and Bosch,L. (1982)

The tRNA-like structure at the 3' terminus of turnip yellow mosaic virus RNA. Differences and similarities with canonical tRNA. *Nucleic Acids Res.*, **10**, 1929-1946.

43. Dam,E., Pleij,K. and Draper,D. (1992) Structural and functional aspects of RNA pseudoknots. *Biochemistry*, **31**, 11665-11676.

44. Brierley,I., Pennell,S. and Gilbert,R.J.. (2007) Viral RNA pseudoknots: versatile motifs in gene expression and replication. *Nat. Rev. Microbiol.*, **5**, 598 - 610.

45. Egli,M., Minasov,G., Su,L. and Rich,A. (2002) Metal ions and flexibility in a viral RNA pseudoknot at atomic resolution. *Proc. Natl. Acad. Sci. U.S.A.*, **99**, 4302-4307.

46. Nixon,P.L., Cornish,P.V., Suram,S.V. and Giedroc,D.P. (2002) Thermodynamic analysis of conserved loop-stem interactions in P1-P2 frameshifting RNA pseudoknots from plant Luteoviridae. *Biochemistry*, **41**, 10665-10674.

47. Chen,X., Kang,H., Shen,L.X., Chamorro,M., Varmus,H.E. and Tinoco,I.,Jr (1996) A characteristic bent conformation of RNA pseudoknots promotes -1 frameshifting during translation of retroviral RNA. *J. Mol. Biol.*, **260**, 479-483.

48. Giedroc,D.P. and Cornish,P.V. (2009) Frameshifting RNA pseudoknots: structure and mechanism. *Virus research*, **139**, 193-208.

49. Wilkinson,S.R. and Been,M.D. (2005) A pseudoknot in the 3' non-core region of the glmS ribozyme enhances self-cleavage activity. *RNA*, **11**, 1788-1794.

50. Montange,R.K. and Batey,R.T. (2008) Riboswitches: emerging themes in RNA structure and function. *Annu. Rev. Biophys*, **37**, 117-133.

51. Gilley,D. and Blackburn,E.H. (1999) The telomerase RNA pseudoknot is critical for the stable assembly of a catalytically active ribonucleoprotein. *Proc. Natl. Acad. Sci. U.S.A.*, **96**, 6621-6625.

52. Wang,C., Le,S.Y., Ali,N. and Siddiqui,A. (1995) An RNA pseudoknot is an essential structural element of the internal ribosome entry site located within the hepatitis C virus 5' noncoding region. *RNA*, **1**, 526-537.

53. Kolupaeva,V.G., Pestova,T.V. and Hellen,C.U. (2000) Ribosomal binding to the internal ribosomal entry site of classical swine fever virus. *RNA*, **6**, 1791-1807.

54. Pestova,T.V., Lomakin,I.B. and Hellen,C.U.T. (2004) Position of the CrPV IRES on the 40S subunit and factor dependence of IRES/80S ribosome assembly. *EMBO Rep.*, **5**, 906-913.

55. Philippe,C., Eyermann,F., Bénard,L., Portier,C., Ehresmann,B. and Ehresmann,C. (1993) Ribosomal protein S15 from Escherichia coli modulates its own translation by trapping the ribosome on the mRNA initiation loading site. *Proc. Natl. Acad. Sci. U.S.A.*, **90**, 4394-4398.

56. Chamorro,M., Parkin,N. and Varmus,H.E. (1992) An RNA pseudoknot and an optimal heptameric shift site are required for highly efficient ribosomal frameshifting on a retroviral messenger RNA. *Proc. Natl. Acad. Sci. U.S.A.*,**89**, 713-717.

57. ten Dam,E., Brierley,I., Inglis,S. and Pleij,C. (1994) Identification and analysis of the pseudoknot-containing gag-pro ribosomal frameshift signal of simian retrovirus-1. *Nucleic Acids Res.*, **22**, 2304-2310.

58. Su,L., Chen,L., Egli,M., Berger,J.M. and Rich,A. (1999) Minor groove RNA triplex in the crystal structure of a ribosomal frameshifting viral pseudoknot. *Nat. Struct. Biol.*, **6**, 285-292.

59. Shen,L.X. and Tinoco,I.,Jr (1995) The structure of an RNA pseudoknot that causes efficient frameshifting in mouse mammary tumor virus. *J. Mol. Biol.*, **247**, 963-978.

60. Chen,X., Chamorro,M., Lee,S.I., Shen,L.X., Hines,J.V., Tinoco,I.,Jr and Varmus,H.E. (1995) Structural and functional studies of retroviral RNA pseudoknots involved in ribosomal frameshifting: nucleotides at the junction of the two stems are important for efficient ribosomal frameshifting. *EMBO J.*, **14**, 842-852.

61. Chen,X., Kang,H., Shen,L.X., Chamorro,M., Varmus,H.E. and Tinoco,I.,Jr (1996) A characteristic bent conformation of RNA pseudoknots promotes -1 frameshifting during translation of retroviral RNA. *J. Mol. Biol.*, **260**, 479-483.

62. Kang,H. and Tinoco,I.,Jr (1997) A mutant RNA pseudoknot that promotes ribosomal frameshifting in mouse mammary tumor virus. *Nucleic Acids Res.*, **25**, 1943-1949.

63. Kang,H., Hines,J.V. and Tinoco,I.,Jr (1996) Conformation of a non-frameshifting RNA pseudoknot from mouse mammary tumor virus. *J. Mol. Biol.*, **259**, 135-147.

64. Morikawa,S. and Bishop,D.H. (1992) Identification and analysis of the gag-pol ribosomal frameshift site of feline immunodeficiency virus. *Virology*, **186**, 389-397.

65. Sung,D. and Kang,H. (1998) Mutational analysis of the RNA pseudoknot involved in efficient ribosomal frameshifting in simian retrovirus-1. *Nucleic Acids Res.*, **26**, 1369 -1372.

66. Du,Z., Holland,J.A., Hansen,M.R., Giedroc,D.P. and Hoffman,D.W. (1997) Base-pairings within the RNA pseudoknot associated with the simian retrovirus-1 gag-pro frameshift site. *J. Mol. Biol.*, **270**, 464-470.

67. Michiels,P.J., Versleijen,A.A., Verlaan,P.W., Pleij,C.W., Hilbers,C.W. and Heus,H.A. (2001) Solution structure of the pseudoknot of SRV-1 RNA, involved in ribosomal frameshifting1. *J. Mol. Biol.*, **310**, 1109-1123.

68. ten Dam,E.B., Verlaan,P.W. and Pleij,C.W. (1995) Analysis of the role of the pseudoknot component in the SRV-1 gag-pro ribosomal frameshift signal: loop lengths and stability of the stem regions. *RNA*, **1**, 146-154.

69. Olsthoorn,R.C., Reumerman,R., Hilbers,C.W., Pleij,C.W. and Heus,H.A. (2010) Functional analysis of the SRV-1 RNA frameshifting pseudoknot. *Nucleic Acids Res.*, **38**, 7665-7672.

70. Wang,Y., Wills,N.M., Du,Z., Rangan,A., Atkins,J.F., Gesteland,R.F. and Hoffman,D.W. (2002) Comparative studies of frameshifting and nonframeshifting RNA pseudoknots: a mutational and NMR investigation of pseudoknots derived from the bacteriophage T2 gene 32 mRNA and the retroviral gag-pro frameshift site. *RNA*, **8**, 981-996.

71. Su,L., Chen,L., Egli,M., Berger,J.M. and Rich,A. (1999) Minor groove RNA triplex in the crystal structure of a ribosomal frameshifting viral pseudoknot. *Nat. Struct. Mol. Biol.*, **6**, 285-292.

72. Egli,M., Minasov,G., Su,L. and Rich,A. (2002) Metal ions and flexibility in a viral RNA pseudoknot at atomic resolution. *Proc. Natl. Acad. Sci. U.S.A.*, **99**, 4302-4307.

73. Pallan,P.S., Marshall,W.S., Harp,J., Jewett,F.C.,3rd, Wawrzak,Z., Brown,B.A.,2nd, Rich,A. and Egli,M. (2005) Crystal structure of a luteoviral RNA pseudoknot and model for a minimal ribosomal frameshifting motif. *Biochemistry*, **44**, 11315-11322.

74. Nixon,P.L., Rangan,A., Kim,Y.-G., Rich,A., Hoffman,D.W., Hennig,M. and Giedroc,D.P. (2002) Solution structure of a luteoviral P1-P2 frameshifting mRNA pseudoknot. *J. Mol. Biol.*, **322**, 621-633.

75. Giedroc,D.P., Cornish,P.V. and Hennig,M. (2003) Detection of scalar couplings involving 2'-hydroxyl protons across hydrogen bonds in a frameshifting mRNA pseudoknot. *J. Am. Chem. Soc*, **125**, 4676-4677.

76. Cornish,P.V., Stammler,S.N. and Giedroc,D.P. (2006) The global structures of a wild-type and poorly functional plant luteoviral mRNA pseudoknot are essentially identical. *RNA*, **12**, 1959-1969.

77. Kim,Y.G., Maas,S., Wang,S.C. and Rich,A. (2000) Mutational study reveals that tertiary interactions are conserved in ribosomal frameshifting pseudoknots of two luteoviruses. *RNA*, **6**, 1157-1165.

78. Nixon,P.L. and Giedroc,D.P. (2000) Energetics of a strongly pH dependent RNA tertiary structure in a frameshifting pseudoknot. *J. Mol. Biol.*, **296**, 659-671.

79. Nixon,P.L., Cornish,P.V., Suram,S.V. and Giedroc,D.P. (2002) Thermodynamic analysis of conserved loop-stem interactions in P1-P2 frameshifting RNA pseudoknots from plant Luteoviridae. *Biochemistry*, **41**, 10665-10674.

80. Chou,M.-Y. and Chang,K.-Y. (2010) An intermolecular RNA triplex provides insight into structural determinants for the pseudoknot stimulator of -1 ribosomal frameshifting. *Nucleic Acids Res.*, **38**, 1676-1685.

81. Cornish,P.V., Hennig,M. and Giedroc,D.P. (2005) A loop 2 cytidine-stem 1 minor groove interaction as a positive determinant for pseudoknot-stimulated -1 ribosomal frameshifting. *Proc. Natl. Acad. Sci. U.S.A.*, **102**, 12694-12699.

82. Cornish,P.V., Stammler,S.N. and Giedroc,D.P. (2006) The global structures of a wild-type and poorly functional plant luteoviral mRNA pseudoknot are essentially identical. *RNA*, **12**, 1959-1969.

83. Cornish,P.V. and Giedroc,D.P. (2006) Pairwise coupling analysis of helical junction hydrogen bonding interactions in luteoviral RNA pseudoknots.

Biochemistry, **45**, 11162-11171.

84. Plant,E.P., Rakauskaite,R., Taylor,D.R. and Dinman,J.D. (2010) Achieving a Golden Mean: Mechanisms by Which Coronaviruses Ensure Synthesis of the Correct Stoichiometric Ratios of Viral Proteins. *J. Virol.*, **84**, 4330-4340.

85. Brierley,I., Digard,P. and Inglis,S.C. (1989) Characterization of an efficient coronavirus ribosomal frameshifting signal: requirement for an RNA pseudoknot. *Cell*, **57**, 537-547.

86. Brierley,I. and Pennell,S. (2001) Structure and function of the stimulatory RNAs involved in programmed eukaryotic-1 ribosomal frameshifting. *Cold Spring Harb. Symp. Quant. Biol.*, **66**, 233-248.

87. Brierley,I., Rolley,N.J., Jenner,A.J. and Inglis,S.C. (1991) Mutational analysis of the RNA pseudoknot component of a coronavirus ribosomal frameshifting signal. *J. Mol. Biol.*, **220**, 889-902.

88. Pleij,C.W., Rietveld,K. and Bosch,L. (1985) A new principle of RNA folding based on pseudoknotting. *Nucleic Acids Res.*, **13**, 1717-1731.

89. Napthine,S., Liphardt,J., Bloys,A., Routledge,S. and Brierley,I. (1999) The role of RNA pseudoknot stem 1 length in the promotion of efficient -1 ribosomal frameshifting. *J. Mol. Biol.*, **288**, 305-320.

90. Liphardt,J., Napthine,S., Kontos,H. and Brierley,I. (1999) Evidence for an RNA pseudoknot loop-helix interaction essential for efficient -1 ribosomal frameshifting. *J. Mol. Biol.*, **288**, 321-335.

91. Cate,J.H., Gooding,A.R., Podell,E., Zhou,K., Golden,B.L., Szewczak,A.A., Kundrot,C.E., Cech,T.R. and Doudna,J.A. (1996) RNA tertiary structure mediation by adenosine platforms. *Science*, **273**, 1696-1699.

92. Kolk,M.H., van der Graaf,M., Wijmenga,S.S., Pleij,C.W., Heus,H.A. and Hilbers,C.W. (1998) NMR structure of a classical pseudoknot: interplay of single- and double-stranded RNA. *Science*, **280**, 434-438.

93. Bredenbeek,P.J., Pachuk,C.J., Noten,A.F., Charité,J., Luytjes,W., Weiss,S.R. and Spaan,W.J. (1990) The primary structure and expression of the second open reading frame of the polymerase gene of the coronavirus MHV-A59; a highly conserved polymerase is expressed by an efficient ribosomal frameshifting mechanism. *Nucleic Acids Res.*, **18**, 1825-1832.

94. Herold,J. and Siddell,S.G. (1993) An "elaborated" pseudoknot is required for high frequency frameshifting during translation of HCV 229E polymerase mRNA. *Nucleic Acids Res.*, **21**, 5838-5842.

95. Thiel,V., Ivanov,K.A., Putics,A., Hertzig,T., Schelle,B., Bayer,S., Weissbrich,B., Snijder,E.J., Rabenau,H., Doerr,H.W., et al. (2003) Mechanisms and enzymes involved in SARS coronavirus genome expression. *J. Gen. Virol.*, **84**, 2305-2315.

96. Brierley,I. and Dos Ramos,F.J. (2006) Programmed ribosomal frameshifting in HIV-1 and the SARS-CoV. *Virus research*, **119**, 29-42.

97. Baranov,P.V., Henderson,C.M., Anderson,C.B., Gesteland,R.F., Atkins,J.F. and Howard,M.T. (2005) Programmed ribosomal frameshifting in decoding the SARS-CoV genome. *Virology*, **332**, 498-510.

98. Plant,E.P., Pérez-Alvarado,G.C., Jacobs,J.L., Mukhopadhyay,B., Hennig,M. and Dinman,J.D. (2005) A Three-Stemmed mRNA Pseudoknot in the SARS Coronavirus Frameshift Signal. *Plos Biol.*, **3**, e172.

99. Su,M.-C., Chang,C.-T., Chu,C.-H., Tsai,C.-H. and Chang,K.-Y. (2005) An atypical RNA pseudoknot stimulator and an upstream attenuation signal for -1 ribosomal frameshifting of SARS coronavirus. *Nucleic Acids Res.*, **33**, 4265-4275.

100. Plant,E.P. and Dinman,J.D. (2008) The role of programmed-1 ribosomal frameshifting in coronavirus propagation. *Frontiers in bioscience: a journal and virtual library*, **13**, 4873.

101. Firth,A.E., Chung,B.Y., Fleeton,M.N. and Atkins,J.F. (2008) Discovery of frameshifting in Alphavirus 6K resolves a 20-year enigma. *Virol. J.*, **5**, 108.

102. Chung,B.Y.-W., Firth,A.E. and Atkins,J.F. (2010) Frameshifting in alphaviruses: a diversity of 3'stimulatory structures. *J. Mol. Biol.*, **397**, 448-456.

103. Paul,C.P., Barry,J.K., Dinesh-Kumar,S.P., Brault,V. and Miller,W.A. (2001) A sequence required for -1 ribosomal frameshifting located four kilobases downstream of the frameshift site. *J. Mol. Biol.*, **310**, 987-999.

104. Barry,J.K. and Miller,W.A. (2002) A -1 ribosomal frameshift element that requires base pairing across four kilobases suggests a mechanism of regulating ribosome and replicase traffic on a viral RNA. *Proc. Natl. Acad. Sci. U.S.A.*,

99, 11133-11138.

105. Tajima,Y., Iwakawa,H.-O., Kaido,M., Mise,K. and Okuno,T. (2011) A long-distance RNA-RNA interaction plays an important role in programmed -1 ribosomal frameshifting in the translation of p88 replicase protein of Red clover necrotic mosaic virus. *Virology*, **417**, 169-178.

106. Mazauric,M.-H., Licznar,P., Prère,M.-F., Canal,I. and Fayet,O. (2008) Apical loop-internal loop RNA pseudoknots: a new type of stimulator of -1 translational frameshifting in bacteria. *J. Biol. Chem.*, **283**, 20421-20432.

107. Pennell,S., Manktelow,E., Flatt,A., Kelly,G., Smerdon,S.J. and Brierley,I. (2008) The stimulatory RNA of the Visna-Maedi retrovirus ribosomal frameshifting signal is an unusual pseudoknot with an interstem element. *RNA*, **14**, 1366-1377.

108. Chou,M.-Y., Lin,S.-C. and Chang,K.-Y. (2010) Stimulation of -1 programmed ribosomal frameshifting by a metabolite-responsive RNA pseudoknot. *RNA*, **16**, 1236-1244.

109. Somogyi,P., Jenner,A.J., Brierley,I. and Inglis,S.C. (1993) Ribosomal pausing during translation of an RNA pseudoknot. *Mol. Cell. Biol.*, **13**, 6931-6940.

110. Kontos,H., Napthine,S. and Brierley,I. (2001) Ribosomal pausing at a frameshifter RNA pseudoknot is sensitive to reading phase but shows little correlation with frameshift efficiency. *Mol. Cell Biol.*, **21**, 8657-8670.

111. Namy,O., Moran,S.J., Stuart,D.I., Gilbert,R.J.C. and Brierley,I. (2006) A mechanical explanation of RNA pseudoknot function in programmed ribosomal frameshifting. *Nature*, **441**, 244-247.

112. Brierley,I., Meredith,M.R., Bloys,A.J. and Hagervall,T.G. (1997) Expression of a coronavirus ribosomal frameshift signal in Escherichia coli: influence of tRNA anticodon modification on frameshifting. *J. Mol. Biol.*, **270**, 360-373.

113. Napthine,S., Vidakovic,M., Girnary,R., Namy,O. and Brierley,I. (2003) Prokaryotic-style frameshifting in a plant translation system: conservation of an unusual single-tRNA slippage event. *EMBO J.*, **22**, 3941-3950.

114. Dulude,D., Baril,M. and Brakier-Gingras,L. (2002) Characterization of the frameshift stimulatory signal controlling a programmed -1 ribosomal frameshift in the human immunodeficiency virus type 1. *Nucleic Acids Res.*,

30, 5094-5102.

115. Staple,D.W. and Butcher,S.E. (2003) Solution structure of the HIV-1 frameshift inducing stem-loop RNA. *Nucleic Acids Res.*, **31**, 4326-4331.

116. Staple,D.W. and Butcher,S.E. (2005) Solution structure and thermodynamic investigation of the HIV-1 frameshift inducing element. *J. Mol. Biol.*, **349**, 1011-1023.

117. Gaudin,C., Mazauric,M.-H., Traïkia,M., Guittet,E., Yoshizawa,S. and Fourmy,D. (2005) Structure of the RNA signal essential for translational frameshifting in HIV-1. *J. Mol. Biol.*, **349**, 1024-1035.

118. Kollmus,H., Honigman,A., Panet,A. and Hauser,H. (1994) The sequences of and distance between two cis-acting signals determine the efficiency of ribosomal frameshifting in human immunodeficiency virus type 1 and human T-cell leukemia virus type II in vivo. *J. Virol.*, **68**, 6087-6091.

119. Kim,Y.G., Maas,S. and Rich,A. (2001) Comparative mutational analysis of cis-acting RNA signals for translational frameshifting in HIV-1 and HTLV-2. *Nucleic Acids Res.*, **29**, 1125-1131.

120. Lucchesi,J., Mäkeläinen,K., Merits,A., Tamm,T. and Mäkinen,K. (2000) Regulation of -1 ribosomal frameshifting directed by cocksfoot mottle sobemovirus genome. *Eur. J. Biochem.*, **267**, 3523-3529.

121. Mäkinen,K., Tamm,T., Naess,V., Truve,E., Puurand,U., Munthe,T. and Saarma,M. (1995) Characterization of cocksfoot mottle sobemovirus genomic RNA and sequence comparison with related viruses. *J. Gen. Virol.*, **76**, 2817-2825.

122. Tamm,T., Suurväli,J., Lucchesi,J., Olspert,A. and Truve,E. (2009) Stem-loop structure of Cocksfoot mottle virus RNA is indispensable for programmed -1 ribosomal frameshifting. *Virus Res.*, **146**, 73-80.

123. Tsuchihashi,Z. and Kornberg,A. (1990) Translational frameshifting generates the gamma subunit of DNA polymerase III holoenzyme. *Proc. Natl. Acad. Sci. U.S.A.*, **87**, 2516-2520.

124. Larsen,B., Gesteland,R.F. and Atkins,J.F. (1997) Structural probing and mutagenic analysis of the stem-loop required for Escherichia coli dnaX ribosomal frameshifting: programmed efficiency of 50%. *J. Mol. Biol.*, **271**,

47-60.

125. Bidou,L., Stahl,G., Grima,B., Liu,H., Cassan,M. and Rousset,J.P. (1997) In vivo HIV-1 frameshifting efficiency is directly related to the stability of the stem-loop stimulatory signal. *RNA*, **3**, 1153-1158.

126. Mäkinen,K., Naess,V., Tamm,T., Truve,E., Aaspõllu,A. and Saarma,M. (1995) The putative replicase of the cocksfoot mottle sobemovirus is translated as a part of the polyprotein by -1 ribosomal frameshift. *Virology*, **207**, 566-571.

127. Mäkeläinen,K. and Mäkinen,K. (2005) Factors affecting translation at the programmed -1 ribosomal frameshifting site of Cocksfoot mottle virus RNA in vivo. *Nucleic Acids Res.*, **33**, 2239-2247.

128. Orlova,M., Yueh,A., Leung,J. and Goff,S.P. (2003) Reverse transcriptase of Moloney murine leukemia virus binds to eukaryotic release factor 1 to modulate suppression of translational termination. *Cell*, **115**, 319-331.

129. Bertrand,C., Prère,M.F., Gesteland,R.F., Atkins,J.F. and Fayet,O. (2002) Influence of the stacking potential of the base 3'of tandem shift codons on -1 ribosomal frameshifting used for gene expression. *RNA*, **8**, 16-28.

130. Baril,M., Dulude,D., Gendron,K., Lemay,G. and Brakier-Gingras,L. (2003) Efficiency of a programmed -1 ribosomal frameshift in the different subtypes of the human immunodeficiency virus type 1 group M. *RNA*, **9**, 1246-1253.

131. Le,S.Y., Shapiro,B.A., Chen,J.H., Nussinov,R. and Maizel,J.V. (1991) RNA pseudoknots downstream of the frameshift sites of retroviruses. *Genet. Anal. Tech. Appl*, **8**, 191-205.

132. Dinman,J.D., Richter,S., Plant,E.P., Taylor,R.C., Hammell,A.B. and Rana,T.M. (2002) The frameshift signal of HIV-1 involves a potential intramolecular triplex RNA structure. *Proc. Natl. Acad. Sci. U.S.A.*, **99**, 5331-5336.

133. Shehu-Xhilaga,M., Crowe,S.M. and Mak,J. (2001) Maintenance of the Gag/Gag-Pol ratio is important for human immunodeficiency virus type 1 RNA dimerization and viral infectivity. *J. Virol.*, **75**, 1834-1841.

134. Telenti,A., Martinez,R., Munoz,M., Bleiber,G., Greub,G., Sanglard,D. and Peters,S. (2002) Analysis of natural variants of the human immunodeficiency virus type 1 gag-pol frameshift stem-loop structure. *J. Virol.*, **76**, 7868-7873.

135. Mazauric,M.-H., Seol,Y., Yoshizawa,S., Visscher,K. and Fourmy,D. (2009) Interaction of the HIV-1 frameshift signal with the ribosome. *Nucleic Acids Res.*, **37**, 7654-7664.

136. Kobayashi,Y., Zhuang,J., Peltz,S. and Dougherty,J. (2010) Identification of a cellular factor that modulates HIV-1 programmed ribosomal frameshifting. *J. Biol. Chem.*, **285**, 19776-19784.

137. Marcheschi,R.J., Mouzakis,K.D. and Butcher,S.E. (2009) Selection and characterization of small molecules that bind the HIV-1 frameshift site RNA. *ACS Chem. Biol.*, **4**, 844-854.

138. Marcheschi,R.J., Tonelli,M., Kumar,A. and Butcher,S.E. (2011) Structure of the HIV-1 Frameshift Site RNA Bound to a Small Molecule Inhibitor of Viral Replication. *ACS Chem. Biol.*, 6, 857-864.

139. Marcheschi,R.J., Staple,D.W. and Butcher,S.E. (2007) Programmed ribosomal frameshifting in SIV is induced by a highly structured RNA stem-loop. *J. Mol. Biol.*, **373**, 652-663.

140. Baril,M., Dulude,D., Steinberg,S.V. and Brakier-Gingras,L. (2003) The frameshift stimulatory signal of human immunodeficiency virus type 1 group O is a pseudoknot. *J. Mol. Biol.*, **331**, 571-583.

141. Olsthoorn,R.C.L., Laurs,M., Sohet,F., Hilbers,C.W., Heus,H.A. and Pleij,C.W.A. (2004) Novel application of sRNA: stimulation of ribosomal frameshifting. *RNA*, **10**, 1702-1703.

142. Howard,M.T., Gesteland,R.F. and Atkins,J.F. (2004) Efficient stimulation of site-specific ribosome frameshifting by antisense oligonucleotides. *RNA*, **10**, 1653-1661.

143. Henderson,C.M., Anderson,C.B. and Howard,M.T. (2006) Antisense-induced ribosomal frameshifting. *Nucleic Acids Res.*, **34**, 4302-4310.